MDPI

Article

Sulphur-Bridged $BAl_5S_5^+$ with 17 Counting Electrons: A Regular Planar Pentacoordinate Boron System

Yuhan Ye [ID]**, Yiqiao Wang, Min Zhang *** [ID]**, Yun Geng** [ID] **and Zhongmin Su**

Institute of Functional Material Chemistry, Faculty of Chemistry & National & Local United Engineering Laboratory for Power Battery, Northeast Normal University, Changchun 130024, China; Yeyh442@nenu.edu.cn (Y.Y.); Wangyq538@nenu.edu.cn (Y.W.); gengy575@nenu.edu.cn (Y.G.); zmsu@nenu.edu.cn (Z.S.)
* Correspondence: mzhang@nenu.edu.cn

Abstract: At present, most of the reported planar pentacoordinate clusters are similar to the isoelectronic substitution of CAl_5^+, with 18 counting electrons. Meanwhile, the regular planar pentacoordinate boron systems are rarely reported. Hereby, a sulphur-bridged $BAl_5S_5^+$ system with a five-pointed star configuration and 17 counting electrons is identified at the global energy minimum through the particle-swarm optimization method, based on the previous recognition on bridged sulphur as the peripheral tactics to the stable planar tetracoordinate carbon and boron. Its outstanding stability has been demonstrated by thermodynamic analysis at 900 K, electronic properties and chemical bonding analysis. This study provides adequately theoretical basis and referable data for its experimental capture and testing.

Keywords: planar pentacoordination; 17 counting electrons; boron multicoordination; sulfur bridging

1. Introduction

Planar hypercoordinate motif is a significant field due to the structural novelty and the rule-breaking traditional recognition on covalent bonding among planar multiatoms. The atomic interaction in the plane configuration exists as a special category, which also possesses a profound impact on the understanding of 2D material structure and the corresponding functional properties. Hence, the plane pentacoordinate carbon (PPC) continues its development and research on the foremost basis of the plane tetracoordination [1]. In addition, understanding the stability exhibited by planar tetracoordinate structures also elucidates further approach to design plane multicoordinate systems [2,3]. Hoffmann et al. [4] firstly theoretically proposed to stabilize plane tetracoordinate carbon (PTC) structure [5–7] with electronic strategy [8] in 1970, and designed planar PTC structure with the lower energy, which attracted extensive attention. With the development of PTC in clusters, planar penta-, hexa- and hepta-coordinate carbon systems as well as other planar multicoordinate carbon (PMC) structures have also been proposed and reported. For example, CB_6^{2-}, CB_7^-, CB_8^-, etc., have been designed or synthesized theoretically or experimentally [9–14].

Due to the unique electronic deficient nature of boron element, planar multicoordinate boron (PMB) structures widely exist in some ionic states of boron clusters and boron-rich systems, which tend to form multicentric bonds between boron atom and other adjacent atoms in nature [15–26]. In 2004, the first global energy minimum (GEM) $BCu_5H_5^-$ with D_{5h} symmetry and bridged hydrogen was first proposed [27]. In 2005, some neutral all-B aromatic clusters with PMB were established according to topological resonance energy. Ref. [28] In 2008, Pei et al. theoretically proposed a series of planar tetra-, penta- and hexa-coordinated carbon-boron mixed clusters [29]. In 2009, Yu et al. proposed the borane cation $B_6H_5^+$ with D_{5h} symmetry and bridged hydrogen, which is another instance of PPB at the GEM and exhibits good aromaticity [30]. Meanwhile, many instances containing PPC are also reported. In 2010, Jimenez-Halla et al. reported the formation of isoelectronic

CAl_4Be and $CAl_3Be_2^-$ clusters by replacing Al atoms in CAl_5^+ with Be and regulating the related charges, where the central carbon acts as the σ receptor and the σ bond possesses a feedback synergistic effect from the C $2p_z$ orbital to the conjugated π bond [31]. In 2015, Guo et al. proposed that $CAl_2Be_3^{2-}$ could realize VDE stabilization through Li^+ and divalent anion complexation [32]. In 2015, Grande-Aztatzi et al. proposed that $CBe_5Li_n^{n-4}$ (n = 2–5) could reduce the electrostatic effect by combining with Li^+ ions [33]. Ding et al. proposed the CAl_4X^+ cluster, CAl_4MX_2 cluster [34] and other transition metal bond cooperation [35]. Until now, most of the planar pentacoordinate clusters fit the isoelectronic substitution of CAl_5^+, namely, the 18 counting electron rule (the total valence electron including the central atom and its adjacent coordinate atoms), which plays a decisive role in providing the corresponding stability [36]. In the latter, researchers found that generally the thermodynamic preference of the 17e/18e counting rule is over the 15e/16e rule.

The GEM structure of B_6S_5 with a plane pentagonal configuration and 18 counting electrons has been identified by our group [37]. Due to the co-existence of π bridge bond and σ bond, the B-S-B-bridged connection effectively realized the combination of electronic strategy and mechanical strategy [37]. Before that, the sulphur-bridged PTC and tetracoordinate boron (PTB) structures were also studied by our group [38,39]. All these studies demonstrate that S atom, as a special bridging element, could help to obtain stabilized planar multicoordinate systems. A five-pointed star configuration of $XAl_5S_5^n$ (X = C, B; n = 0, +1, +2) was considered in this study, with B and C as the central atom and S as the peripheral bridged atoms. Through the structure search and the subsequent reconfirmation, the $BAl_5S_5^+$ structure was finally identified as an excellent system with a five-pointed star configuration at its GEM and 17 counting electrons. Its outstanding stability has been further verified by the corresponding orbital analysis, thermodynamic analysis, and so on. The details are provided in the following parts.

2. Results and Discussion

2.1. Structure and Stability of $XAl_5S_5^n$ (X = C, B; n = 0, +1, +2) Clusters

The initially generated structures were all identified at B3LYP/6-31G for $XAl_5S_5^n$ (X = C, B; n = 0, +1, +2) clusters through the particle-swarm optimization method. The obtained structures with no imaginary frequency were further optimized at B3LYP/def2-TZVP level. Finally, single-point calculations were carried out for the four isomers with the lowest energies at the CCSD/6-31G(d) level and with ZPE corrections at the same level.

The GEM structures of four systems with PPC or PPB are all shown in Figure 1, and their other low-lying structures are shown in Figure S1 in the Supplementary Materials. The energy of PPC D_{5h} $CAl_5S_5^{2+}$ with 17 counting electrons is 14.68 kJ/mol lower than that of the second-lowest energy structure. Meanwhile, the energy of PPB D_{5h} $BAl_5S_5^+$ with 17 counting electrons is 28.90 kJ/mol lower than that of the second-lowest energy structure. These two systems at their GEM structures with 18 counting electrons are also with quasi-planar pentacoordinate central atom. However, their symmetries both drop to C_1. Other information about the low-lying structures of these systems is all given in Figure S1 in the Supplementary Materials.
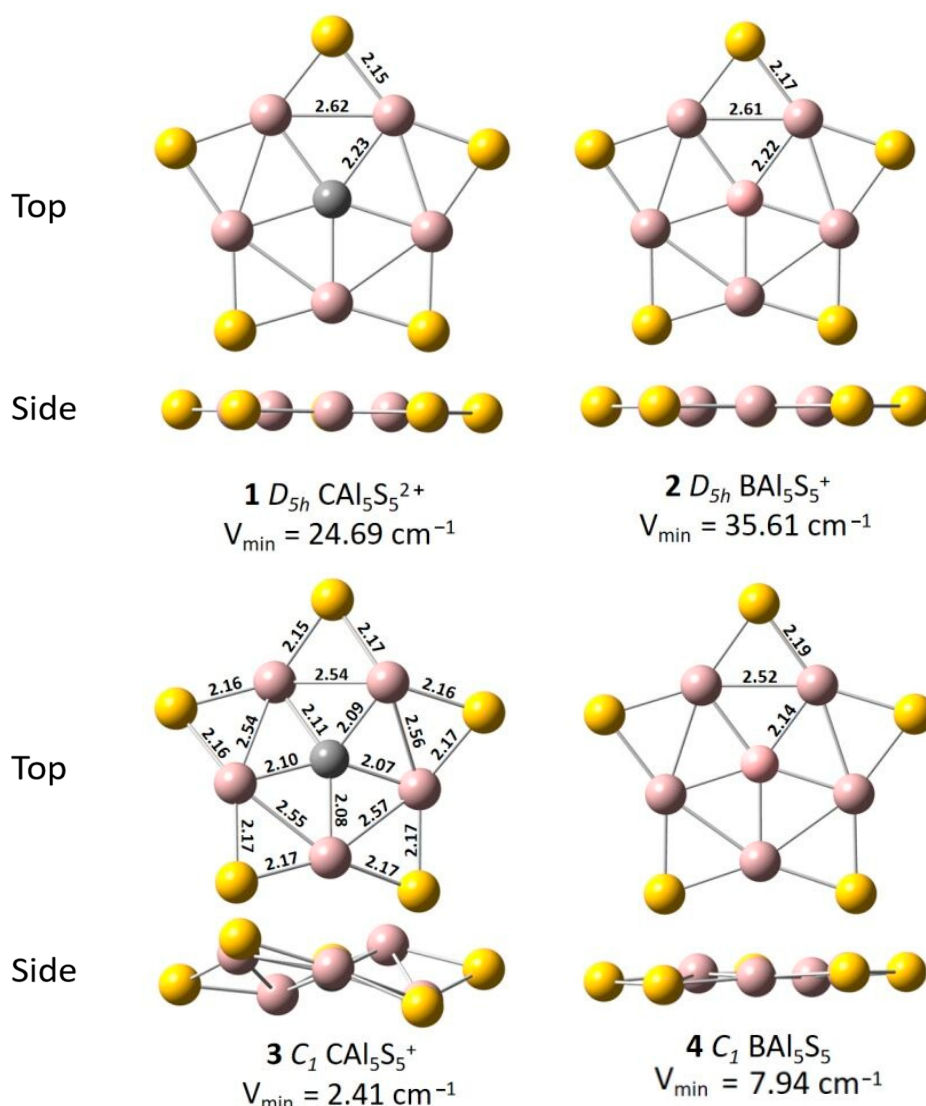
Figure 1. The Optimized Structures and Bond Lengths for XAl_5S_5 (X = C, B; n = 0, +1, +2) clusters and their lowest frequencies at CCSD/6-31G(d) level.

Then, Born–Oppenheimer molecular dynamics (BOMD) simulations [40] of four GEM structures were performed over 15 ps at ambient temperature, 600 K and 900 K for the evaluation on their dynamic stability. The PPB D_{5h} $BAl_5S_5^+$ with 17 counting electrons can keep its structural integrity even at 900 K (Figure 2), which is extremely robust against isomerization and decomposition. Its RMSDs fluctuate relatively small, suggesting its good kinetic stability. In contrast, The PPC D_{5h} $CAl_5S_5^{2+}$ with 17 counting electrons can keep its structural integrity at 600 K (Figure S2 in the Supplementary Materials). The other two systems with 18 counting electrons also can keep their structural integrity at 298 K (Figure S2 in the Supplementary Materials). These data demonstrate: firstly, D_{5h} $BAl_5S_5^+$ with the highest stability; secondly, the systems with 17 counting electrons are more stable than those with 18 counting electrons in our systems.
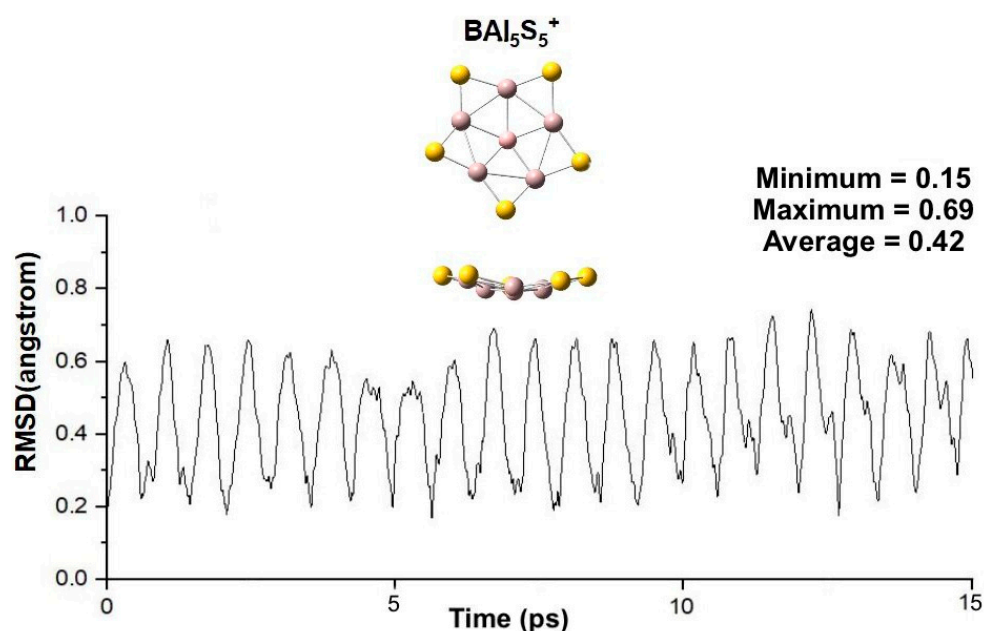
Figure 2. Root-mean-square deviations (RMSD) of $BAl_5S_5^+$ during Born–Oppenheimer molecular dynamics (BOMD) simulations at 900 K. The final snapshot of the structure is also shown here.

2.2. Electronic Properties and NBO Analysis on $CAl_5S_5^+$, $CAl_5S_5^{2+}$, BAl_5S_5, $BAl_5S_5^+$

To investigate and understand the reason why $BAl_5S_5^+$ possesses the best stability among these systems, the electronic properties and bonding analysis on CAl_5S_5 and BAl_5S_5 with 17 and 18 counting electrons are discussed here. Table 1 lists their NPA and WBI bond orders obtained from NBO analysis. Through further structural analysis, it can be found that the central C and B are negatively charged, the aluminum is positively charged, and the peripheral sulfur is negatively charged. The negative–positive–negative distribution of electrons is beneficial to their stability. According to bond level analysis, the Al-Al Wiberg bond level is very weak (the WBI_{Al-Al} values are all below 0.14), indicating that their interatomic bonding is very weak. The key factor to stabilize the PPC and PPB atoms is the C-Al and B-Al bonding, as well as the stability of the Al-S-Al bond in the periphery. This also indicates that S, as a bridged atom, plays an important role in maintaining the stability of the plane structure.

Table 1. Important NPA charges and Wiberg Bond Indices (WBIs) of $CAl_5S_5^+$, $CAl_5S_5^{2+}$, BAl_5S_5, $BAl_5S_5^+$.

	$CAl_5S_5^+$ (18e)	$CAl_5S_5^{2+}$ (17e)		BAl_5S_5 (18e)	$BAl_5S_5^+$ (17e)
Q_C	−2.50	−1.87	Q_B	−2.56	−0.63
Q_{Al}	1.42/1.43/1.44	1.40	Q_{Al}	1.31	0.66
Q_S	−0.72/−0.73/−0.74	−0.63	Q_S	−0.80	−0.34
WBI_C	2.43	2.06	WBI_B	3.36	2.80
WBI_{Al}	2.47–2.51	2.51	WBI_{Al}	2.66	2.61
WBI_S	1.99–2.02	2.10	WBI_S	1.92	1.99
WBI_{C-Al}	0.40–0.45	0.36	WBI_{B-Al}	0.60	0.50
WBI_{Al-Al}	0.10	0.10	WBI_{Al-Al}	0.14	0.12
WBI_{Al-S}	0.89–0.93	0.96	WBI_{Al-S}	0.85	0.91

The total WBI bond levels of C atoms in electron $CAl_5S_5^{2+}$ (17e) and 18 electron $CAl_5S_5^+$ (17e) are 2.06 and 2.43, respectively. Similarly, the total WBI bond levels of B atoms in electron $BAl_5S_5^+$ (17e) and 18 electron BAl_5S_5 (18e) are 2.80 and 3.36, respectively. This indicates that the interaction between central B atom and adjacent Al atoms is much

stronger than that between central C atom and adjacent Al atoms. Meanwhile, the dynamic stability of $BAl_5S_5^+$ is best, although its WBI total value is not the highest one.

Localized orbital locator (LOL) [41] analysis can well reflect the electron distribution in the whole system (Figure 3). It is clearly easy to see that the electron distribution is symmetrically distributed in $BAl_5S_5^+$. No region with electron density is over 0.6e there, indicating that electron repulsion is relatively small. To clarify, the difference of electron repulsion caused the last counting electron. The uneven bonding and unevenly distributed electron in other systems must result in the reduction in the stability. Furthermore, the existence of the higher electron density in the small area also produces stronger electron repulsion. In addition, the electron distribution and the corresponding energy of the six highest-occupied π MOs in $BAl_5S_5^+$ and BAl_5S_5 are shown in Figures S3 and S4 in the Supplementary Materials, which is a very important factor to maintain the planar structure. Clearly, the similar degenerate π MOs exists, but the energies of the orbital energies of BAl_5S_5 are very high compared to those α energies f $BAl_5S_5^+$. These also can elucidate why $BAl_5S_5^+$ is the best one among all the investigated systems. That is consistent with the previous BOMD analysis (Figure 2).
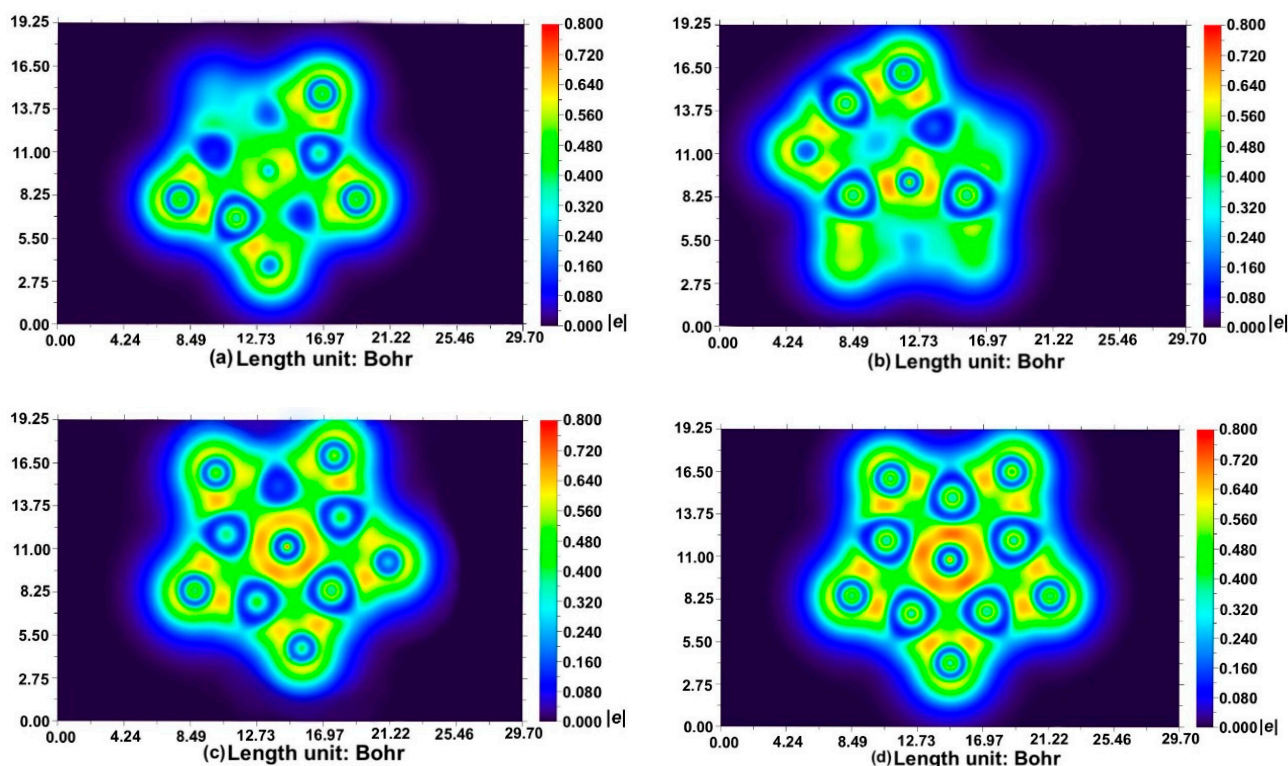

Figure 3. Localized orbital locator (LOL) analysis of (**a**) $CAl_5S_5^+$, (**b**) $CAl_5S_5^{2+}$, (**c**) BAl_5S_5, (**d**) $BAl_5S_5^+$.

2.3. Chemical Bonding on the PPB $BAl_5S_5^+$ Cluster

The internal bonding mode and electron distribution characteristics can be intuitively understood by semi-localized AdNDP analysis. After the previous stability exploration, the AdNDP analysis on $BAl_5S_5^+$ is executed (Figure 4). The analysis clearly shows the lone pair of five S atoms, the two-center–two-electron (2c–2e) σ bond between Al-S atoms and the three-center–two-electron (3c–2e) π bond between Al-S-Al atoms. The 5π bonds fit the rule of Hückel aromatics (2 × 2 + 1), which is one of the factors that stabilize the whole structure. In addition, the central atom B of the planar pentacoordination is stabilized by five delocalized bonds: three delocalized 6c–2e σ bonds and one delocalized π single electron in the 6c–2e bond (electron-occupied number is about 1.1e). The 3σ bonds indicate the σ contribution to the central atom B, while the inner single-electron π bond overlaps

weak with the outer 5π bonds. The semi-localized AdNDP analysis showed that the electron repulsion in the system was very weak, which made $BAl_5S_5^+$ exhibit good stability at 17 electrons.
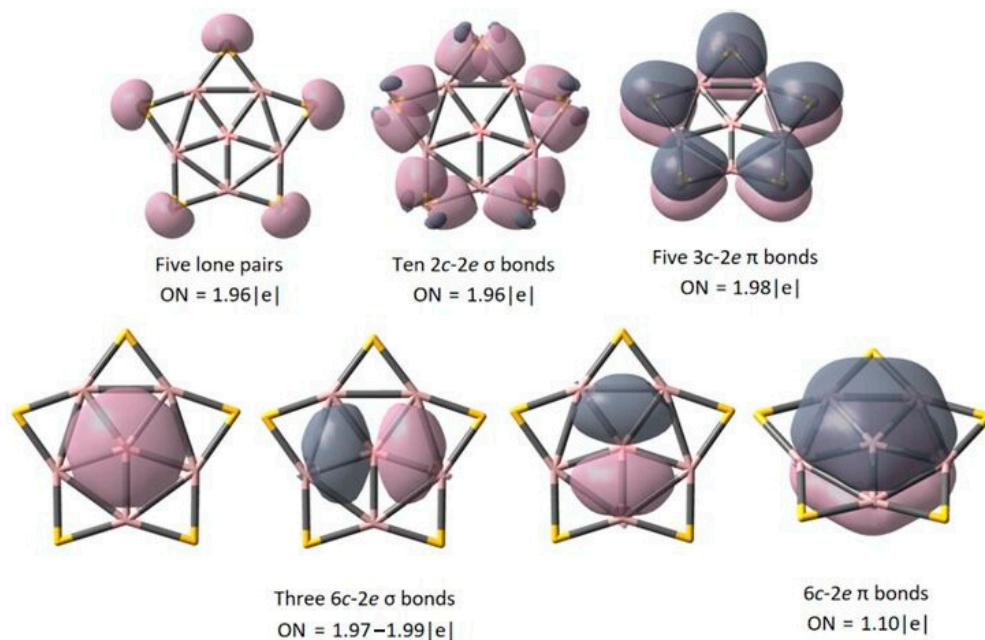

Figure 4. AdNDP analysis of D_{5h} $BAl_5S_5^+$.

In order to confirm the conclusion of aromaticity obtained by AdNDP analysis, we calculated the NICs values for the structure of $BAl_5S_5^+$. The NICS value over central B atom at 1 Å and 2 Å are both negative (−12.80 ppm and −3.13 ppm), indicating its excellent aromaticity. The NICS values at other positions are also shown in Figure 5. The aromatic existence in $BAl_5S_5^+$ makes its structure stable, which provides a further explanation for the previous kinetic and thermodynamic stability.
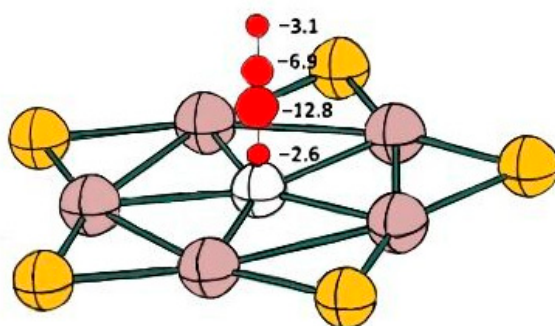

Figure 5. NICS value analysis of D_{5h} $BAl_5S_5^+$.

3. Computational Methodology

The global minimum structural search of all the $XAl_5S_5{}^n$ (X = C, B; *n* = 0, +1, +2) clusters were conducted with the particle-swarm optimization (PSO) method [42], as implemented in the CALYPSO [39] code. More than 1000 stationary points were generated and searched for each of the species. All the calculations, including optimization and the corresponding analysis, were executed using the Gaussian 09 package [43]. Restricted calculation is used for closed-shell systems, and unrestricted calculation is used for open-shell systems and odd-electron systems, and the energy differences caused by spin multiplicity are also considered. These PPB species, together with other low-lying states, were re-optimized and the harmonic vibrational frequencies analysis at the hybrid B3LYP functional in connection

with def2-TZVP basis set to further ensure they are the ground states [44]. Finally, these GEM clusters of $XAl_5S_5{}^n$ were analyzed using Natural Bond Orbital (NBO) 3.0 in Gaussian 09 for obtaining natural population analysis (NPA), Wiberg bond indices (WBIs). Adaptive natural density partitioning (AdNDP) [44] analyses were operated at the same level using the Multifwn3.3.8 program [41].

4. Conclusions

A $BAl_5S_5{}^+$ system with a five-pointed star configuration and 17 counting electrons is identified at the global energy minimum.

The sulphur-bridged planar structure of $BAl_5S_5{}^+$ with a five-pointed star configuration at the global energy minimum is identified through the particle-swarm optimization method and possesses the best stability among the investigated systems of $XAl_5S_5{}^n$ (X = C, B; n = 0, +1, +2). By calculating BOMD, $BAl_5S_5{}^+$ endures the best stability at 900 K. The following analysis on the electronic property and chemical bonding clearly interprets the contribution from peripheral S-bridged connection and the 17 counting electrons. This study provides adequately theoretical basis and referable data for its experimental capture and testing.

Supplementary Materials: The following are available online, Figure S1: The optimized structures of the four lowest isomers of PPC/B and quasi-PPC systems at B3LYP/def2-TZVP and the corresponding single-point energies at CCSD/6-31g(d) and the lowest frequency, Figure S2: Born–Oppenheimer molecular dynamics (BOMD) simulations at different temperatures and their root-mean-square deviations (RMSD) for four systems. Figure S3: The α electron profile and the corresponding energy of the 6 highest-occupied π MOs of $BAl_5S_5{}^+$. Figure S4: The electron profile and the corresponding energy of the 6 highest-occupied π MOs of BAl_5S_5. Table S1: The important information on the GEM structures of PPC/B and quasi-PPC systems at B3LYP/def2-TZVP level.

Author Contributions: Y.Y. and Y.W. executed the theoretical simulation and wrote the first version of the manuscript, M.Z. designed the research project and wrote the final version of this article, Y.G. and Z.S. joined this project and the discussion of this study. All authors have read and agreed to the published version of the manuscript.

Institutional Review Board Statement: Not applicable.

Informed Consent Statement: Not applicable.

Data Availability Statement: Data are contained within this article.

Conflicts of Interest: The authors declare no conflict of interest.

Sample Availability: Not applicable.

References

1. Wang, Y.; Li, Y.F.; Chen, Z.F. Planar Hypercoordinate Motifs in Two-Diemensional Materials. *Acc. Chem. Res.* **2020**, *1*, 887–895. [CrossRef]
2. Vassilev-Galindo, V.; Pan, S.J.; Donald, K.; Merino, G. Planar pentacoordinate carbons. *Nat. Rev. Chem.* **2018**, *2*, 0114. [CrossRef]
3. Zhu, C.Y.; Lv, H.F.; Qu, X.; Zhang, M.; Wang, J.Y.; Wen, S.Z.; Li, Q.; Geng, Y.; Su, Z.M.; Wu, X.J.; et al. TMC (TM = Co, Ni, and Cu) monolayers with planar pentacoordinate carbon and their potential applications. *J. Mater. Chem. C* **2019**, *7*, 6406–6413. [CrossRef]
4. Hoffmann, R.; Alder, R.W.; Wilcox, C.F. Planar tetracoordinate carbon. *J. Am. Chem. Soc.* **1970**, *92*, 4992–4993. [CrossRef]
5. Collins, J.B.; Dill, J.D.; Jemmis, E.D.; Apeloig, Y.; von Rague Schleyer, P.; Seeger, R.; Pople, J.A. Stabilization of planar tetracoordinate carbon. *J. Am. Chem. Soc.* **1976**, *98*, 5419–5427. [CrossRef]
6. Cui, Z.-H.; Shao, C.-B.; Gap, S.-M.; Ding, Y.-H. Pentaatomic planar tetracoordinate carbon molecules [XCAl$_3$]^q [(X,q) = (B,−2), (C,−1), (N,0)] with C–X multiple bonding. *Phys. Chem. Chem. Phys.* **2010**, *12*, 13637–13645. [CrossRef] [PubMed]

7. Tsutsumi, K.; Ogoshi, S.; Nishiguchi, S.; Kurosawa, H. Synthesis, Structure, and Reactivity of Neutral η3-Propargylpalladium Complexes. *J. Am. Chem. Soc.* **1998**, *120*, 1938–1939. [CrossRef]

8. Wang, Z.X.; Schleyer, P.R. Construction principles of „hyparenes": Families of molecules with planar pentacoordinate carbons. *Science* **2001**, *292*, 2465–2469. [CrossRef]

9. Wang, L.-S.; Boldyrev, A.I.; Li, X.; Simon, J. Experimental Observation of Pentaatomic Tetracoordinate Planar Carbon-Containing Molecules. *J. Am. Chem. Soc.* **2000**, *122*, 7681–7687. [CrossRef]

10. Wang, L.-M.; Huang, W.; Averkiev, B.B.; Boldyrev, A.I.; Wang, L.-S. CB_7^-: Experimental and Theoretical Evidence against Hypercoordinate Planar Carbon. *Angew. Chem. Int. Ed.* **2007**, *46*, 4550–4553. [CrossRef] [PubMed]

11. Averkiev, B.B.; Dmitry, Y.Z.; Wang, L.-M.; Huang, W.; Wang, L.-S.; Boldyrev, A.I. Carbon Avoids Hypercoordination in CB_6^-, CB_6^{2-}, and $C_2B_5^-$ Planar Carbon−Boron Clusters. *J. Am. Chem. Soc.* **2008**, *130*, 9248–9250. [CrossRef]

12. Averkiev, B.B.; Wang, L.-M.; Huang, W.; Wang, L.-S.; Boldyrev, A.I. Experimental and theoretical investigations of CB_8^-: Towards rational design of hypercoordinated planar chemical species. *Phys. Chem. Chem. Phys.* **2009**, *11*, 9840–9849. [CrossRef]

13. Wu, Y.B.; Jiang, J.L.; Lu, H.G.; Wang, Z.X.; Perez-Peralta, N.; Islas, R.; Contreras, M.; Merino, G.; Wu, I.C.; von Rague Schleyer, P. Starlike Aluminum–Carbon Aromatic Species. *Chem. Eur. J.* **2011**, *17*, 714–719. [CrossRef]

14. Wu, Y.B.; Yuan, C.-X.; Yang, P. The $C_6B_{12}^{2-}$ complex: A beautiful molecular wheel containing a ring of six planar tetracoordinate carbon atoms. *J. Mol. Struc. Theochem* **2006**, *765*, 35–38. [CrossRef]

15. Aldridge, S.; Downs, A.J. Hydrides of the Main-Group Metals: New Variations on an Old Theme. *Chem. Rev.* **2001**, *101*, 3305–3366. [CrossRef] [PubMed]

16. Minkin, V.I.; Minyaev, R.M.; Hoffmann, R. Non-classical structures of organic compounds: Unusual stereochemistry and hypercoordination. *Russ. Chem. Rev.* **2002**, *71*, 869–892. [CrossRef]

17. Erhardt, S.; Frenking, G.; Chen, Z. Aromatic Boron Wheels with More than One Carbon Atom in the Center: C2B8, C3B93+, and C5B11+. *Angew. Chem.* **2005**, *117*, 1102–1106. [CrossRef]

18. Keese, R. Carbon Flatland: Planar Tetracoordinate Carbon and Fenestranes. *Chem. Rev.* **2006**, *106*, 4787–4808. [CrossRef] [PubMed]

19. Islas, R.; Heine, T.; Ito, K.; Schleyer, P.R.; Merino, G. Boron Rings Enclosing Planar Hypercoordinate Group 14 Elements. *J. Am. Chem. Soc.* **2007**, *129*, 14767–14774. [CrossRef]

20. Liao, Y.; Cruz, C.L.; Schleyer, P.R.; Chen, Z. Many M©Bn boron wheels are local, but not global minima. *Phys. Chem. Chem. Phys* **2012**, *14*, 14898–14904. [CrossRef] [PubMed]

21. Sergeeva, A.P.; Popov, I.A.; Piazza, Z.A.; Li, W.-L.; Romanescu, C.; Wang, L.-S.; Boldyrev, A.I. Understanding Boron through Size-Selected Clusters: Structure, Chemical Bonding, and Fluxionality. *Acc. Chem. Res.* **2014**, *47*, 1349–1358. [CrossRef] [PubMed]

22. Yang, L.-M.; Ganz, E.; Chen, Z.; Wang, Z.-X.; von Rague Schleyer, P. Four Decades of the Chemistry of Planar Hypercoordinate Compounds. *Angew. Chem. Int. Ed.* **2015**, *54*, 9468–9501. [CrossRef]

23. Wang, L.-S. Photoelectron spectroscopy of size-selected boron clusters: From planar structures to borophenes and borospherenes. *Int. Rev. Phys. Chem.* **2016**, *35*, 69–142. [CrossRef]

24. Guo, J.-C.; Feng, L.-Y.; Dong, C.; Zhai, H.-J. Planar Pentacoordinate versus Tetracoordinate Carbons in Ternary CBe_4Li_4 and $CBe_4Li_4^{2-}$ Clusters. *J. Phys. Chem. A* **2018**, *122*, 8370–8376. [CrossRef] [PubMed]

25. Guo, J.-C.; Feng, L.-Y.; Zhai, H.-J. Ternary CBe4Au4 cluster: A 16-electron system with quasi-planar tetracoordinate carbon. *Phys. Chem. Chem. Phys.* **2018**, *20*, 6299–6306. [CrossRef]

26. Miao, C.Q.; Guo, J.C.; Li, S.D. M@B_9 and M@B_{10} molecular wheels containing planar nona-and deca-coordinate heavy group 11, 12, and 13 metals (M=Ag, Au, Cd, Hg, In, Tl). *Sci. China Chem.* **2009**, *52*, 900–904. [CrossRef]

27. Li, S.-D.; Miao, C.-Q.; Ren, G.-M. D5h Cu5H5X: Pentagonal Hydrocopper Cu5H5 Containing Pentacoordinate Planar Nonmetal Centers (X = B, C, N, O). *Eur. J. Inorg. Chem.* **2004**, *2004*, 2232–2234. [CrossRef]

28. Aihara, J.-I.; Kanno, A.H.; Ishida, T. Aromaticity of Planar Boron Clusters Confirmed. *J. Am. Chem. Soc.* **2005**, *127*, 13324–13330. [CrossRef] [PubMed]

29. Pei, Y.; Zeng, X.C. Probing the Planar Tetra-, Penta-, and Hexacoordinate Carbon in Carbon−Boron Mixed Clusters. *J. Am. Chem. Soc.* **2008**, *130*, 2580–2592. [CrossRef]

30. Yu, H.-L.; Sang, R.-L.; Wu, Y.-Y. Structure and Aromaticity of B6H5+ Cation: A Novel Borhydride System Containing Planar Pentacoordinated Boron. *J. Phys. Chem. A* **2009**, *113*, 3382–3386. [CrossRef] [PubMed]

31. Jimenez-Halla, J.O.C.; Wu, Y.-B.; Wang, Z.-X.; Islas, R.; Heine, T.; Merino, G. CAl4Be and CAl3Be2−: Global minima with a planar pentacoordinate carbon atom. *Chem. Commun.* **2009**, *46*, 8776–8778. [CrossRef] [PubMed]

32. Wu, Y.-B.; Duan, Y.; Lu, H.-G.; Li, S.-D. CAl2Be32– and Its Salt Complex LiCAl2Be3–: Anionic Global Minima with Planar Pentacoordinate Carbon. *J. Phys. Chem. A* **2012**, *116*, 3290–3294. [CrossRef]

33. Li, S.-D.; Guo, Q.-L.; Miao, C.-Q.; Ren, G.-M. Investigation on Transition-Metal Hydrometal Complexes M_nH_nC with Planar Coordinate Carbon Centers by Density Functional Theory. *Wuli Huaxue Xuebao* **2007**, *23*, 743–745.

34. Cui, Z.-H.; Sui, J.-J.; Ding, Y.-H. How can carbon favor planar multi-coordination in boron-based clusters? Global structures of $CB_xE_y^{2-}$ (E = Al, Ga, x + y = 4). *Phys. Chem. Chem. Phys.* **2015**, *17*, 32016–32022. [CrossRef] [PubMed]

35. Zhang, X.-Y.; Ding, Y.-H. Computational prediction of a global planar penta-coordinate carbon structure CAl4Ga+. *Comput. Theor. Chem.* **2014**, *1048*, 18–24. [CrossRef]

36. Merino, G.; Mendez-Rojas, M.; Vela, A.; Heine, T. Recent advances in planar tetracoordinate carbon chemistry. *J. Comput. Chem.* **2006**, *28*, 362–372. [CrossRef]

37. Wang, Y.Q.; Wang, C.; Liu, X.M.; Zhang, M.; Geng, Y.; Zhao, L. Planar Tetracoordinate Boron and Pentacoordinate Boron in B_6S_5 Clusters. *Chem. J. Chin. Univ.* **2020**, *41*, 1625–1630.

38. Zhang, X.; Wang, Y.; Geng, Y.; Zhang, M.; Su, Z. Theoretical study on the stable plane CAl_4 structure of sulfur—aluminum bridge bond. *Chem. J. Chin. Univ.* **2018**, *39*, 2485–2491.

39. Wang, Y.; Lv, J.; Zhu, L.; Ma, Y. CALYPSO: A method for crystal structure prediction. *Comput. Phys. Commun.* **2012**, *183*, 2063–2070. [CrossRef]

40. VandeVondele, J.; Krack, M.; Mohamed, F.; Parrinello, M.; Chassaing, T.; Hutter, J. Quickstep: Fast and accurate density functional calculations using a mixed Gaussian and plane waves approach. *Comput. Phys. Commun.* **2005**, *167*, 103–128. [CrossRef]

41. Lu, T.; Chen, F. Multiwfn: A multifunctional wavefunction analyzer. *J. Comput. Chem.* **2012**, *33*, 580–592. [CrossRef] [PubMed]

42. Wang, Y.; Lv, J.; Zhu, L.; Ma, Y. Crystal structure prediction via particle-swarm optimization. *Phys. Rev. B* **2010**, *82*, 094116. [CrossRef]

43. Frisch, M.J.; Trucks, G.W.; Schlegel, H.B.; Scuseria, G.E.; Robb, M.A.; Cheeseman, J.R.; Montgomery, J.A.; Vreven, J.; Kudin, T.K.N.; Burant, J.C.; et al. *Gaussian 09, Revision A.02*; Gaussian Inc.: Wallingford, CT, USA, 2009.

44. Weigend, F.; Ahlrichs, R. Balanced basis sets of split valence, triple zeta valence and quadruple zeta valence quality for H to Rn: Design and assessment of accuracy. *Phys. Chem. Chem. Phys.* **2005**, *7*, 3297–3305. [CrossRef] [PubMed]